

Fattening Chips: Hypertrophy, Feeding, and Fasting of Human White Adipocytes In Vitro

Benjamin D. Pope, Curtis R. Warren, Madeleine Dahl, Christina V. Pizza, Douglas E. Henze, Nina R. Sinatra, Grant M. Gonzalez, Huibin Chang, Qihan Liu, Aaron L. Gliberman, John P. Ferrier Jr., Chad A. Cowan and Kevin Kit Parker

5

Supplementary Materials:

Supplementary Tables

Table S1 | Source Information for Human Preadipocytes Used in this Study

Name	Type	Gender	Age	BMI	Biopsy	Type 2 Diabetic	Vendor	Lot Numbers
Visceral	Primary	F	55	35	Omentum	N	Zen-Bio	OMM020216C
Subcutaneous	Primary	F	46,51	25,24	Abdomen, Breast	N	PromoCell	394Z027.1 423Z037.1
Diabetic visceral	Primary	F	59	45	Mesentery	Y	Zen-Bio	DMSNM072005
ESC derived	HUES9 embryonic stem cell derived	F	N/A	N/A	N/A	N/A	N/A	N/A

10

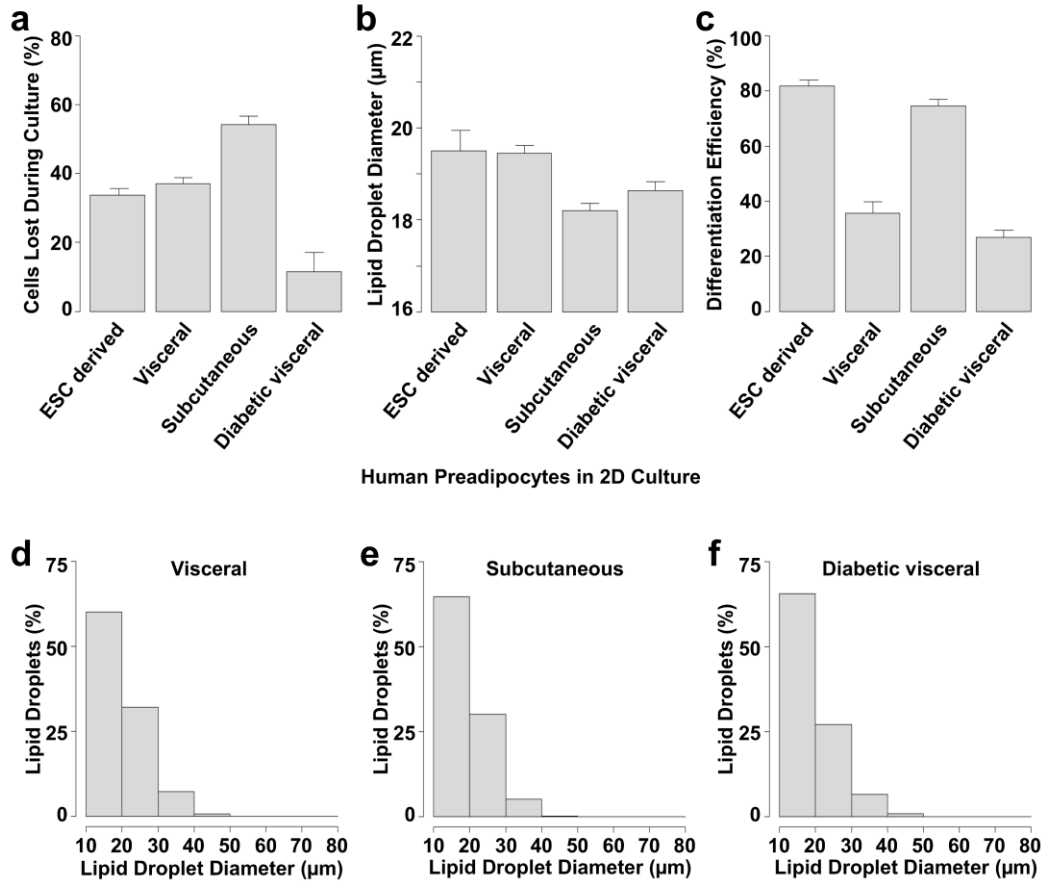
Supplementary Movies

15 **Movie S1 | In vitro differentiated adipocytes detach from conventional two-dimensional culture surfaces.** The focal plane is adjusted from culture surface to air-liquid interface to visualize floating adipocytes.

Adipocyte Hypertrophy

20

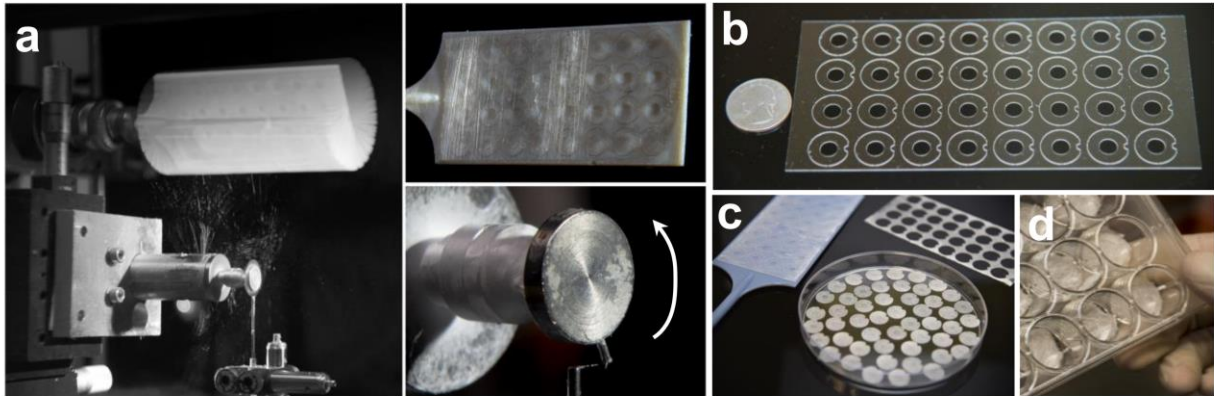
25



30

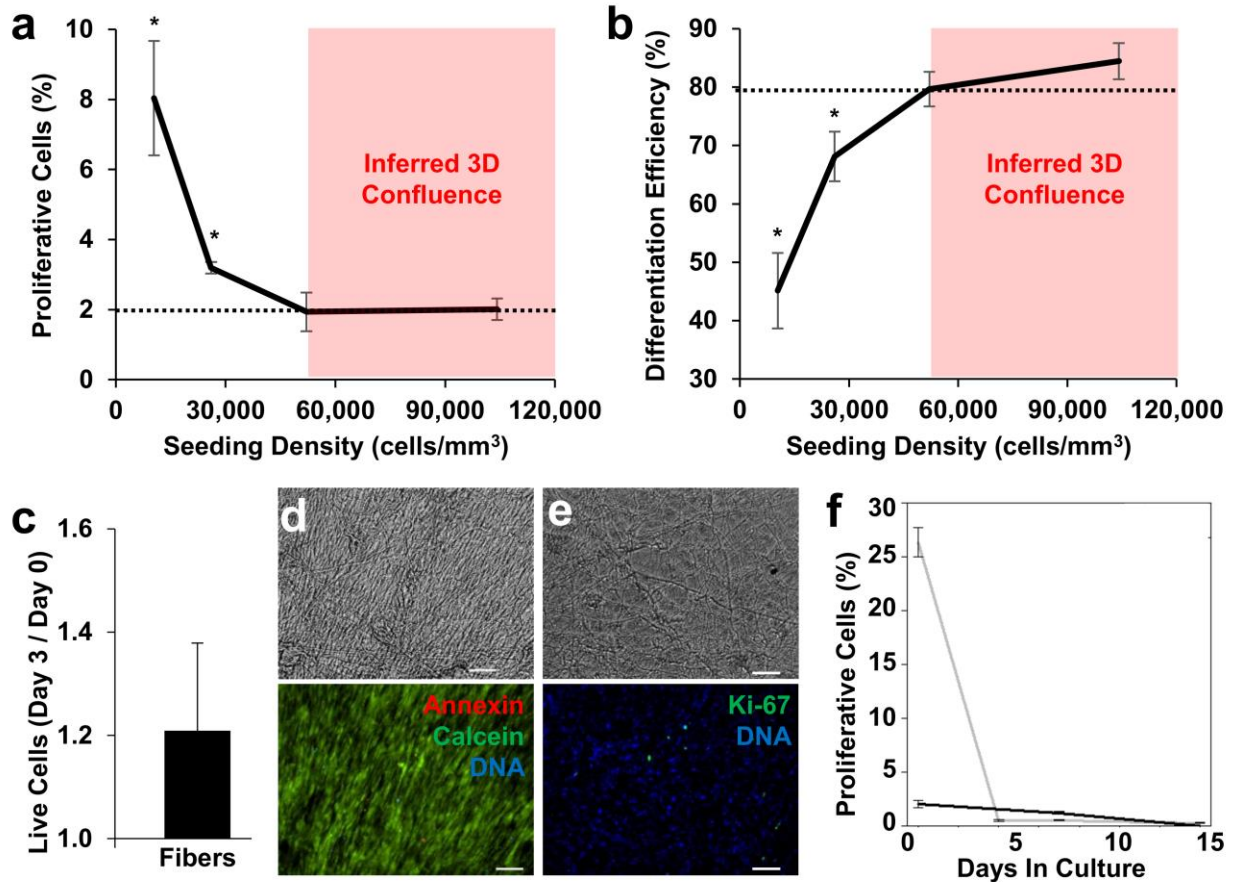
35

Figure S1 | Adipocyte detachment, size, and differentiation efficiency in conventional culture. a-c. Percentage decrease of cell number (panel a), average lipid droplet diameter (panel b), and differentiation efficiency (panel c) for differentiations of four different preadipocyte sources. Cell loss and lipid droplet size measurements were taken after 30 days of culture, while differentiation efficiency was calculated after 21 days. Means and standard errors are shown from 4-11 differentiations per preadipocyte source. **d-f.** Distributions of the lipid droplet diameters ($n = 22,834$ for visceral, $273,414$ for subcutaneous, and $16,736$ for diabetic visceral, respectively) within adipocytes differentiated in vitro using the indicated preadipocyte sources after 31 days of culture.



40 **Figure S2 | Manufacture of fiber networks for multi-well culture.** **a.** Timelapse photograph of fiber network fabrication by pull spinning (left). Still photographs of the bristle during formation of a single fiber (bottom right) and the mandrel during fiber collection (top right) are also shown. **b.** Photograph of an array of multi-well inserts that were laser cut from polycarbonate sheets for fiber collection during pull spinning. **c.** Photograph of an array coated with fibers on a collection mandrel (top left), a fiber coated array following laser excision of inserts (top right), and excised fiber coated inserts in a 15 cm dish (middle). **d.** Photograph of fiber networks installed in a 12-well plate.

Adipocyte Hypertrophy



45

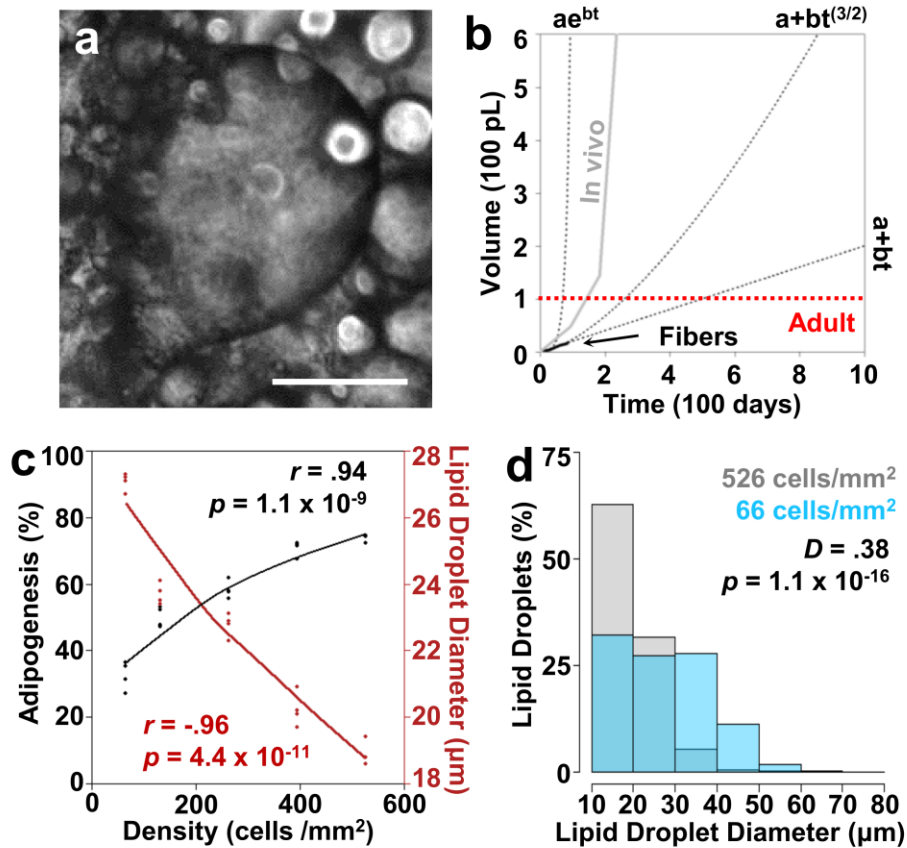
50

55

60

Figure S3 | Testing of fiber networks for multi-well culture. **a.** Proliferation in ESC derived human preadipocyte cultures on fiber networks on the same day as seeding as a function of seeding density. Significant increases ($n = 3$ wells per time point; $p < .05$; Wilcoxon rank sum test) in proliferation relative to the minimum (dotted horizontal line) are indicated by asterisks. **b.** Day 21 differentiation efficiency in ESC derived human preadipocyte cultures on fiber networks as a function of seeding density. Significant decreases ($n = 3$ wells per time point; $p < .05$; Wilcoxon rank sum test) in efficiency relative to that of confluent 2D cultures (dotted horizontal line) are indicated by asterisks. **c.** Quantification of total cell number as a ratio of cells counted after 3 days of culture to the number of cells originally seeded. **d.** Phase contrast (top) and fluorescence (bottom) micrographs of stained live preadipocytes on a fiber network after 3 days of culture. Cells were stained by active transport and metabolism of cytosolic Calcein AM (green) while dead cells lacking intact membranes were stained by 4',6-diamidino-2-phenylindole (DAPI, blue), a membrane impermeable DNA stain. Annexin V (red) was also used as a marker of apoptosis. Scale bar is 50 μm . **e.** Phase contrast (top) and fluorescence (bottom) micrographs of fixed preadipocytes on a fiber network after 1 day of culture. Proliferation indicated by Ki-67 immunofluorescence (green) with Hoechst nuclear stain (blue). Initial differences in proliferation were likely due to temporary differences in confluence between the two-dimensional well and the three-dimensional fibers. Scale bar is 50 μm . **f.** Time course of proliferation in preadipocyte cultures on fiber networks (black) or conventional well plates (gray). Means and standard errors of three replicate cultures per time point and condition are shown. ESC derived human preadipocytes were used in all panels.

65



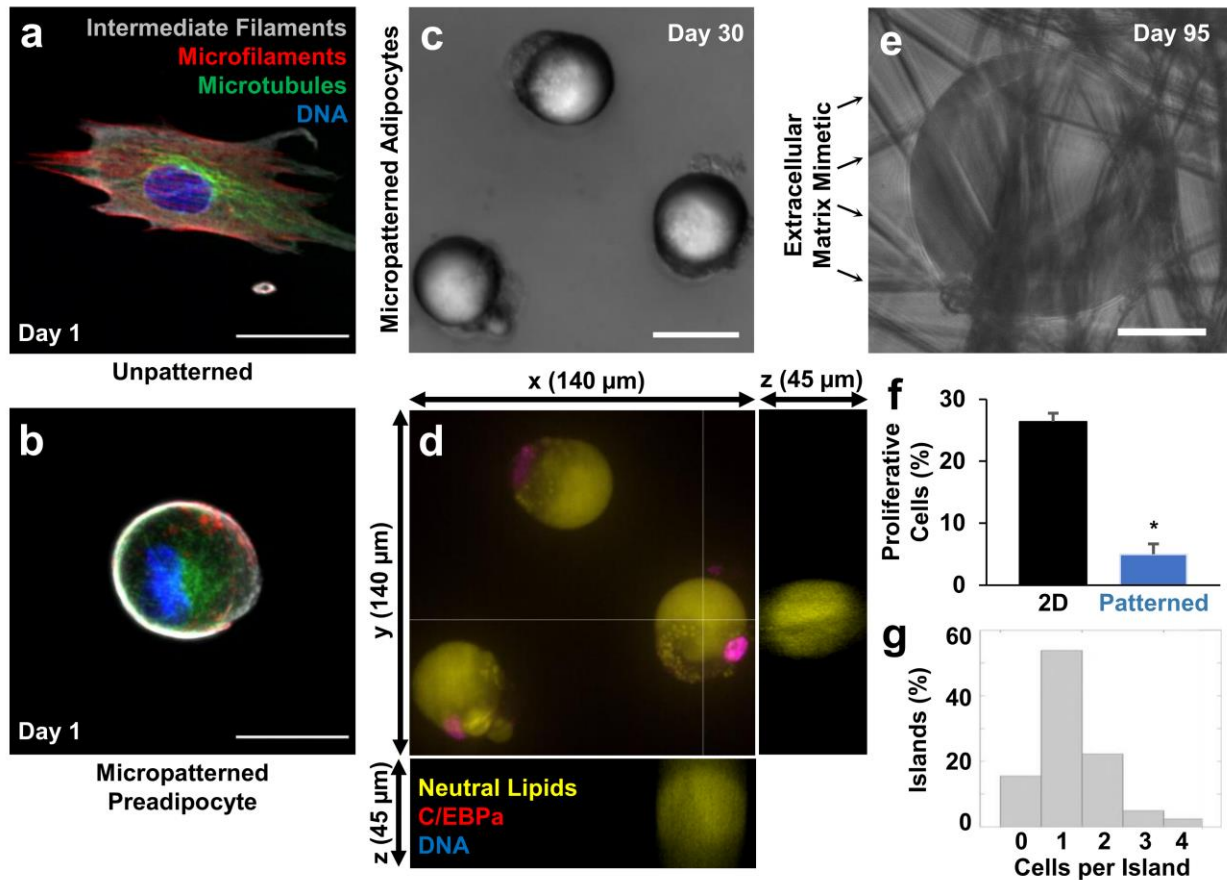
70

Figure S4 | Rates of adipocyte hypertrophy depend upon culture density. **a.** Phase contrast micrograph of a 220 μm diameter adipocyte differentiated in vitro on a fiber network. Scale bar is 100 μm . **b.** Empirical adipocyte size measurements from developing and postnatal humans (in vivo, solid gray curve) and from differentiations on fiber networks (solid black curve) are plotted as a function of time together with fitted exponential [ae^{bt}], linear [$a+bt$], and power law [$a+bt^{(3/2)}$] mathematical models, where “a” is initial volume, “t” is time, and “b” is a fitting parameter. While an exponential model can be fitted to data from conventional methods, data from differentiations on fibers beyond 30 days suggest an alternative growth model is more appropriate. A red dashed horizontal line indicates the volume of a cell that is 58 μm in diameter (i.e. 100 pL). **c.** Adipocyte differentiation efficiency (black) and lipid droplet diameter (red) measured within adipocytes differentiated in vitro from ESC derived human preadipocytes by conventional methods after 31 days of culture are plotted as functions of culture density. Individual data points from four differentiations and loess smoothed curves are shown. Pearson’s correlation (r) and corresponding p-values (p) are also shown. **d.** Distributions of lipid droplet diameters within adipocytes differentiated in vitro by conventional methods after 30 days of culture at culture densities of either 66 (semi-transparent blue) or 526 (gray) cells per mm^2 ($n = 24,856$ and $205,403$ cells, respectively). The Kolmogorov-Smirnov statistic (D) for the distributions and the corresponding p-value (p) are also shown.

75

80

85



95 **Figure S5 | Circular cell patterning under fiber networks accelerates adipocyte hypertrophy by promoting adipogenesis in preadipocytes at low seeding density.** a-b. Fluorescence micrographs of unrestricted (panel a) and patterned (panel b) primary human subcutaneous preadipocytes after 1 day of culture. Vimentin (gray), filamentous actin (red), and α tubulin (green) are shown with nuclei (blue). Destabilization of microfilaments promotes adipogenesis and can be seen on the circular pattern. Scale bars are 25 μm . c-d. Phase contrast (panel c) and confocal fluorescence (panel d) micrographs of adipocytes generated after 30 days of culture by the micropatterning and matrix mimicy (M&MM) method. Transcription factor C/EBP α (red) is shown with lipid droplets (yellow) and nuclei (blue). Orthogonal views of the z planes indicated by crossing lines over the bottom right adipocyte demonstrate the cell's spherical shape. e. Phase contrast micrograph of a 156 μm diameter adipocyte after 95 days of culture by the micropatterning and matrix mimicy (M&MM) method. Scale bar is 100 μm . f. Expression of proliferation marker Ki-67 as a percentage of cells on the same day as seeding in conventional 2D culture (n = 69,574 cells from six different wells) versus on the M&MM chip ("Patterned"; n = 201 cells from four wells; $p = 9.5 \times 10^{-3}$; Wilcoxon rank sum test). ESC derived human preadipocytes were used. g. Distribution of the number of cells (Hoechst stained nuclei) per island (n = 1,115 cells from two wells) using primary human subcutaneous preadipocytes after 1 day of culture.

100

105